Tracking Unstable Turing Patterns through Mixed-Mode Spatiotemporal Chaos

Valery Petrov,[1] Stephane Metens,[2] Pierre Borckmans,[2] Guy Dewel,[2] and Kenneth Showalter[1,2]
[1]*Department of Chemistry, West Virginia University, Morgantown, West Virginia 26506-6045*
[2]*Service de Chimie Physicque, Université Libre de Bruxelles, Campus Plaine, 1050 Bruxelles, Belgium*
(Received 19 May 1995)

A method is presented for stabilizing and tracking unstable Turing patterns in reaction-diffusion systems. The Gray-Scott model is used to simulate a chemical system exhibiting spatiotemporal chaos arising from the interaction between Turing and Hopf bifurcations. The local behavior of the unstable pattern is first approximated with a single-input, single-output linear model constructed from a time series. A recursive control algorithm is then used to stabilize and track the unstable pattern by monitoring a single point in space and making small adjustments to a global parameter.

PACS numbers: 82.40.Bj, 05.45.+b

Stabilization techniques based on the Ott-Grebogi-Yorke (OGY) [1] method have been highly successful for controlling low-dimensional systems [2]. Controlling spatiotemporal systems remains a challenge, however, because the unstable states in such systems are typically high dimensional, involving multiple stable and unstable modes. Some spatiotemporal systems can be controlled with simple methods, such as propagating fronts with highly correlated spatial modes [3], convectively unstable systems [4], or systems that are stabilized at multiple sites [5]. Periodic behavior in myocardium tissue [6] and hippocampal brain tissue [7] has been stabilized by deducing the stable and unstable manifold positions from time delay maps and applying appropriate perturbations. Simple control approaches typically fail, however, when the unstable state has more than one unstable direction. Auerbach *et al.* [8] and Romerias *et al.* [9] have generalized the OGY method for stabilizing systems with many stable and unstable manifolds.

We recently proposed a control method that combines the OGY approach with the classical control routines of single-input, single-output (SISO) systems [10]. The method was applied to stabilize unstable periodic orbits and steady states of the Kuramoto-Sivashinsky equation. In this Letter we demonstrate how the method can be applied to stabilize and track unstable Turing patterns through mixed-mode spatiotemporal chaos.

A recent study by De Wit, Dewel, and Borckmans [11] has shown how spatiotemporal chaos arises in reaction-diffusion systems near a Turing-Hopf codimension-2 bifurcation point. The interaction between the Turing and Hopf modes in the vicinity of such a point may result in *mixed-mode* spatiotemporal oscillations. We use the Gray-Scott cubic autocatalysis model [12] to simulate a 1D reaction-diffusion system exhibiting mixed-mode spatiotemporal chaos.

The governing equations of the reaction-diffusion Gray-Scott model [13] have the form

$$\frac{\partial \alpha}{\partial t} = \delta \nabla^2 \alpha + \frac{(1-\alpha)}{T_{\mathrm{res}}} - \alpha\beta^2,$$
$$\frac{\partial \beta}{\partial t} = \nabla^2 \beta + \frac{(\beta_0-\beta)}{T_{\mathrm{res}}} + \alpha\beta^2 - k_2\beta, \qquad (1)$$

where $\nabla^2 = \partial^2/\partial x^2$ in the 1D case, and $\delta = D_\alpha/D_\beta$ is the ratio of the reactant and autocatalyst diffusion coefficients. The diffusion terms are calculated using finite differences, and no-flux boundary conditions are imposed at $x = 0$ and $x = 300$. We concentrate on the behavior of this system for the specific parameter values $\beta_0 = \frac{1}{15}$, $\kappa_2 = \frac{1}{40}$, and $\delta = 4.6$.

The bifurcation diagram corresponding to varying the remaining parameter T_{res} is shown in Fig. 1. The steady-state locus yields a "mushroom" pattern with two ranges of multiple steady states, one at low T_{res} and one at high T_{res}. In addition, there is a Hopf bifurcation point along the uppermost branch of the mushroom. As the residence time is increased the homogeneous steady state loses stability at this point and a stable limit cycle emerges, with homogeneous oscillations displayed throughout the medium. As T_{res} is further increased, a Turing-Hopf mixed mode appears through a subharmonic instability. This new solution loses its stability and gives rise to complex spatiotemporal behavior.

Over the range $214.8 < T_{\mathrm{res}} < 242$, a Turing pattern with a typical stationary periodic concentration profile is observed. The maximum in $\alpha(x)$ of the spatial oscillations as a function of T_{res} is shown by the dotted line in Fig. 1. At high T_{res} the system settles back onto the limit cycle of the homogeneous oscillations. At low T_{res}, the Turing branch becomes unstable as it enters the complex spatiotemporal region.

We now present a general method for controlling multidimensional systems using scalar time series (see Ref. [10] for a detailed description), which we will use for stabilizing the unstable Turing pattern through the range of complex behavior. Multidimensional systems are typically monitored by the observation of a single experi-

0031-9007/95/75(15)/2895(4)$06.00 © 1995 The American Physical Society

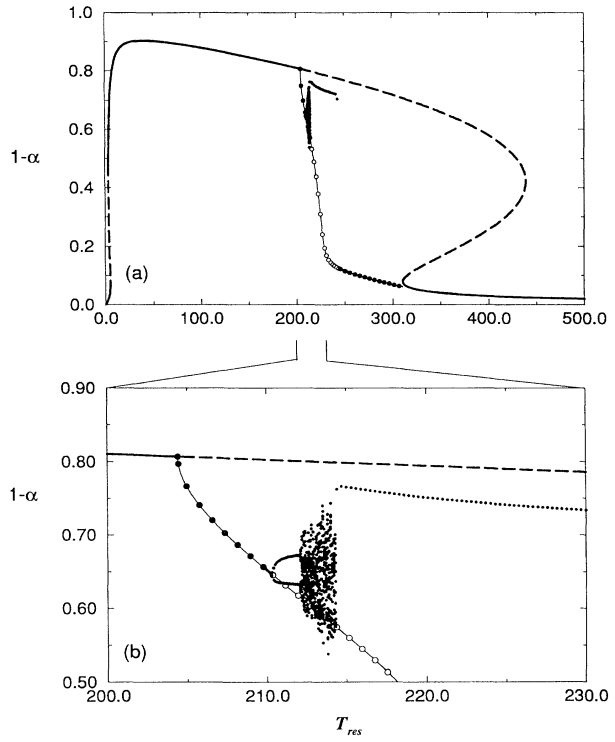

FIG. 1. (a) Homogeneous stable (solid line) and unstable (dashed line) steady state of the Gray-Scott model as a function of T_{res}. The circles show the locus of the stable (●) and unstable (○) uniform period-1 orbit. (b) Blowup of (a) near the region of complex spatiotemporal oscillations. The dots represent the minimum in $1 - \alpha$ along the spatial profile of the Turing pattern for $T_{\text{res}} > 214.8$ and show the minimum in $1 - \alpha$ oscillations at $x = 0$ for $T_{\text{res}} < 214.8$.

mentally accessible variable. Although the corresponding time series is a projection of the system dynamics in phase space, control can be achieved by using a set of time-delayed observations.

When an m-dimensional system is sampled with a time interval τ, the coordinate ξ_i along the ith eigenvector moves according to

$$\xi_i(t + \tau) - \xi_i^F = \lambda_i[\xi_i(t) - \xi_i^F], \quad i = 1, \ldots, m, \quad (2)$$

where $\vec{\xi}^{\text{F}}$ is the steady-state position and λ_i is the ith eigenvalue of the time-discretized system. We assume that there is an experimentally accessible parameter p which alters the dynamics in such a way that the fixed point moves when a small perturbation δp is applied. Following the application of such a perturbation, the system evolves according to the position of the shifted fixed point,

$$\vec{\xi}^F(p + \delta p) = \vec{\xi}^F(p) + \frac{\partial \vec{\xi}^F}{\partial p}\,\delta p. \quad (3)$$

For simplicity, we assume that $\vec{\xi}^F(p) = 0$. We also assume that the perturbation δp is kept constant from t to $t + \tau$ and is equal to $u(t + \tau)$. Equations (2) and (3) can then be combined to give the equations of motion in the presence of the perturbations:

$$\xi_i(t + \tau) = \lambda_i \xi_i(t) + (1 - \lambda_i)\frac{\partial \xi_i^F}{\partial p}\,u(t + \tau),$$
$$i = 1, \ldots, m. \quad (4)$$

If we introduce a time-shift operator $\hat{\mathbf{q}}$, such that $\hat{\mathbf{q}}^j(y(t)) = y(t + j\tau)$, we can rewrite Eq. (4) as

$$\xi_i(t) = \frac{\hat{\mathbf{q}}(1 - \lambda_i)}{\hat{\mathbf{q}} - \lambda_i}\frac{\partial \xi_i^F}{\partial p}\,u(t), \qquad i = 1, \ldots, m. \quad (5)$$

In an experimental setting, we typically monitor some observable $y(t)$ that is a linear combination of the system variables:

$$y(t) = \sum_{i=1}^{m} c_i \xi_i(t). \quad (6)$$

We assume that $c_i \neq 0$ for all unstable eigenvectors, i.e., the unstable behavior *is observable* using $y(t)$. To combine Eqs. (5) and (6), we introduce the coefficients that are proportional to the shift of the steady state:

$$\gamma_i = c_i(1 - \lambda_i)\frac{\partial \xi_i^F}{\partial p}. \quad (7)$$

The relation between perturbation $u(t)$ and observable $y(t)$ can then be written as

$$y(t) = \sum_{i=1}^{m} \frac{\gamma_i \hat{\mathbf{q}}}{\hat{\mathbf{q}} - \lambda_i}\,u(t). \quad (8)$$

Equation (8) is a transfer function between the system input $u(t)$ and output $y(t)$. It models the response of the m-dimensional system to a perturbation. The common denominator form of this equation is

$$y(t) = \frac{b_1\hat{\mathbf{q}}^m + b_2\hat{\mathbf{q}}^{m-1} + \cdots + b_m\hat{\mathbf{q}}^1}{\hat{\mathbf{q}}^m + a_1\hat{\mathbf{q}}^{m-1} + \cdots + a_m\hat{\mathbf{q}}^0}\,u(t). \quad (9)$$

The denominator of the transfer function is a polynomial whose roots are eigenvalues of the linearized system. Following Ref. [14], we denote the denominator of Eq. (9) as $\hat{\mathbf{A}}(q)$ and the numerator as $\hat{\mathbf{B}}(q)$. Equation (9) can now be rewritten in a compact form:

$$\hat{\mathbf{A}}(q)y(t) = \hat{\mathbf{B}}(q)u(t). \quad (10)$$

To find the coefficients from an experimental time series we express Eq. (10) as

$$y(n) = \sum_{i=1}^{m} -a_i y(n - i) + b_i u(n + 1 - i), \quad (11)$$

where $y(j) = y(t + j\tau)$ and $u(j) = u(t + j\tau)$. The coefficients a_i and b_i of Eq. (11) are calculated directly from the sampled time series of $u(t)$ and $y(t)$ as a solution of the linear system [10]. Rearranging Eq. (9) into the partial-fraction form of Eq. (8) gives the coefficients γ_i. Each γ_i tells how far the steady state is displaced along the ith eigenvector following the perturbation and, in many cases, allows an estimation of the effective system dimension. Specifically, if the system dimension is overestimated, then for some $i, |\gamma_i| \ll \min(|\gamma_j|_{j \neq i})$, the ith eigendirection can be discarded.

To stabilize a linear system modeled with Eq. (10), controlling perturbations are calculated as a linear function of n delayed readings and $n - 1$ previous perturbations:

$$\hat{\mathbf{L}}(q)u(t) = \hat{\mathbf{P}}(q)y(t), \tag{12}$$

where $\hat{\mathbf{L}}(q)$ and $\hat{\mathbf{P}}(q)$ are the mth order polynomials of successive powers of the time-shift operator [15]. The control law coefficients l_i and p_i determine the behavior of the closed-loop system according to Eqs. (10) and (12):

$$[\hat{\mathbf{A}}(q) \cdot \hat{\mathbf{L}}(q) - \hat{\mathbf{B}}(q)\hat{\mathbf{P}}(q)]y(t) = \hat{\mathbf{A}}^*(q)y(t) = 0, \tag{13}$$

where the center dot indicates multiplication of the polynomials. According to Eq. (13), $2m - 1$ eigenvalues of the closed-loop system can be set to any value with an appropriate choice of the coefficients l_i and p_i (the pole-placement technique) [10,15]. We require all eigenvalues of $\hat{\mathbf{A}}^*(q)$ to be stable (modulus < 1) so the system converges toward the fixed point.

We now demonstrate the stabilization of unstable Turing patterns with the 1D reaction-diffusion Gray-Scott model. The linearized recursive model of the dynamical system is obtained by imposing *random* perturbations onto the global parameter T_{res} at regular sampling intervals $\tau = 50.0$. Values of α at the system boundary $x = 0$ along with the applied perturbations produce a set of data pairs $(y(i), u(i))$. This set is fitted to Eq. (11) and the recursive coefficients a_i, b_i are calculated using the method of singular value decomposition. The coefficients l_i, p_i that determine the controlling perturbations are found as a solution of the linear system defined by Eq. (13).

Tracking an unstable state requires adaptive control, where the values of a_i and b_i are redetermined each step with the system in the vicinity of the state. Once the tracking is initiated, small random perturbations are added to the continuously applied controlling perturbations to interrogate the system. This technique allows the control coefficients to be updated every time the bifurcation parameter is changed.

To initialize the tracking procedure it is necessary to determine a solution for some value of the bifurcation parameter, find the effective dimensionality of the system in the linear region of that solution, and calculate the control coefficients. A suitable starting point can be found in the vicinity of a bifurcation that destabilizes the system. A stable Turing pattern with nine half-wavelengths is exhibited by Eq. (1) for $T_{\text{res}} = 217.0$. The appropriate value of m was determined during the initialization. It was found for $m = 4$ that γ_4 corresponds to $\lambda_4 \approx 0$, and it is 2 orders of magnitude smaller than the remaining γ_i. Therefore, the fourth (highly attractive) mode gives a negligible contribution to the time series readings and can be discarded. An effective system dimension of three was used to stabilize the Turing pattern.

One step of the tracking routine is illustrated in Fig. 2. The identification of the linearized dynamics is carried out during the first 50 iterations. Once the system identification is completed (at $i = 50$), the bifurcation parameter T_{res} is changed to a new value. Provided the change in T_{res} is sufficiently small, the old control parameters l_i and p_i are close to the new values and the system is stabilized. As shown in Fig. 2, the system converges to the new steady state following the change in T_{res} (at $i = 51$). The identification routine is then repeated after the convergence reaches a preset limit.

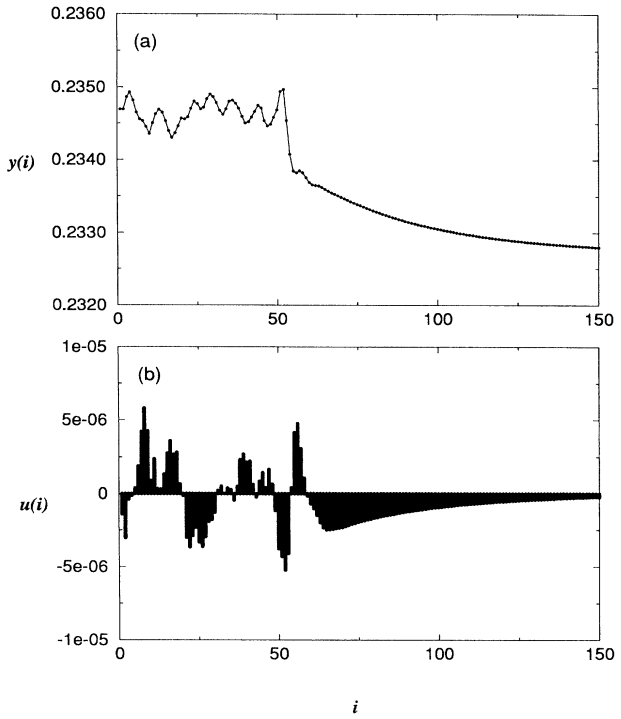

FIG. 2. Identification and tracking of unstable Turing pattern at $T_{\text{res}} = 214.5$. (a) Value of $y(i) = \alpha$ collected at $x = 0$; (b) the corresponding adjustments of $u(i) = T_{\text{res}}$.

The position of the stabilized Turing pattern was recorded for each step of the bifurcation parameter and is shown in Fig. 3(a). The three eigenvalues (Floquet multipliers) of the unstable Turing pattern are calculated as the roots of the denominator of Eq. (10). The absolute values of these roots are shown in Fig. 3(b). The two complex eigenvalues correspond to the uniform oscillatory mode that becomes unstable at $T_{\text{res}} = 214.8$ as T_{res} is decreased. The third (real) eigenvalue approaches unity as the residence time approaches the Turing bifurcation at $T_{\text{res}} = 210.7$. When T_{res} is below this value, the tracking algorithm switches to the stabilization of the uniform unstable steady state, as shown in Fig. 3(a).

The application of the tracking algorithm results in a qualitative change in behavior at the expense of very small perturbations to the system. The unstable Turing pattern is maintained throughout the region where the autonomous Gray-Scott system exhibits spatiotemporal chaos. Space-time plots of the autonomous and controlled systems at $T_{\text{res}} = 214.5$ are compared in Fig. 4.

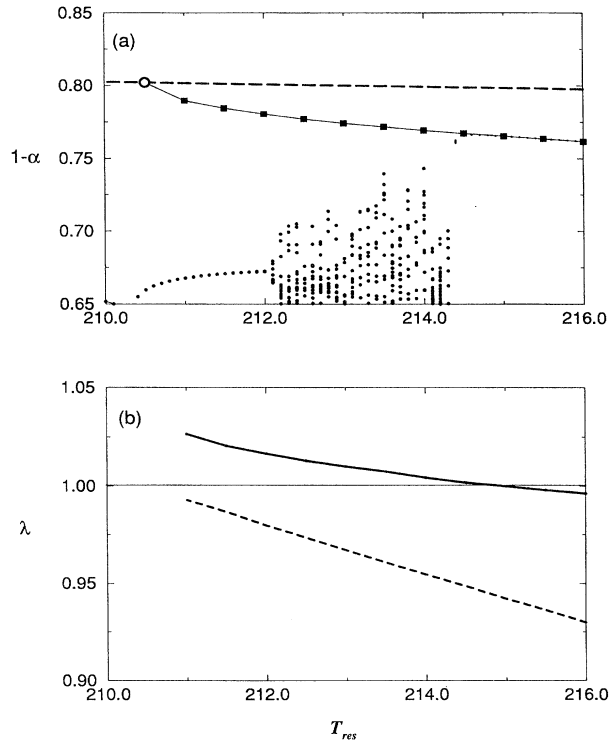

FIG. 3. Bifurcation diagram showing (a) the autonomous system response (●) and the tracked unstable Turing pattern (■). Open circle (○) shows stabilized homogeneous steady state. Unstable steady state (dashed line) is also shown. (b) Modulus of complex conjugate eigenvalues (solid line) and real eigenvalue (dashed line) corresponding to slowest decaying mode as a function of T_{res}.

A spatially distributed system has an infinite number of degrees of freedom; however, only two modes of the Turing pattern become unstable to produce the mixed-mode chaos. The third, stable mode appears as a response to the homogeneous perturbations. We note that the method can be readily applied to control higher dimensional states, and a four-cell front of the Kuramoto-Sivashinsky equation with three stable and six unstable modes has been stabilized [10].

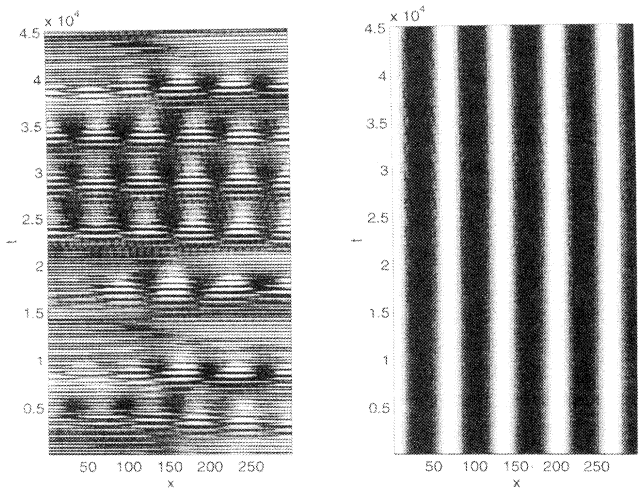

FIG. 4. Space-time plot of autonomous (left) and controlled (right) Gray-Scott system at $T_{\text{res}} = 214.5$.

When coupled with the tracking technique, the stabilization algorithm provides a model-independent continuation method for bifurcation analysis of experimental systems. We anticipate that the approach can be extended to control spatially distributed chemical and biological processes in two- and three-dimensional media by monitoring and perturbing the system at multiple locations separated by the characteristic correlation length.

K. S. is grateful to Professor Grégoire Nicolis for his hospitality at the Service de Chimie Physique, Université Libre de Bruxelles. We thank Anne De Wit for helpful discussions. K. S. thanks the National Science Foundation (Grant No. CHE-9222616), the Office of Naval Research (Grant No. N00014-95-1-0247), and the Petroleum Research Fund (Grant No. 29565-AC6) for supporting this research. P. B. and G. D. received support from the FNRS (Belgium).

[1] E. Ott, C. Grebogi, and J. A. Yorke, Phys. Rev. Lett. **64**, 1196 (1990).

[2] For reviews see T. Shinbrot, C. Grebogi, E. Ott, and J. A. Yorke, Nature (London) **363**, 411 (1993); W. L. Ditto and L. Pecora, Sci. Am., Aug. 1993, p. 78; E. Ott and M. Spano, Phys. Today **48**, No. 5, 34 (1995); K. Showalter, Chem. Br. **31**, 202 (1995).

[3] V. Petrov, M. F. Crowley, and K. Showalter, J. Chem. Phys. **101**, 6606 (1994).

[4] D. Auerbach, Phys. Rev. Lett. **72**, 1184 (1994); G. A. Johnson, M. Locher, and E. R. Hunt, Phys. Rev. E **51**, R1625 (1995).

[5] J. A. Sepulchre and A. Babloyantz, Phys. Rev. E **48**, 945 (1993).

[6] A. Garfinkel, M. L. Spano, W. L. Ditto, and J. N. Weiss, Science **257**, 1230 (1992).

[7] S. J. Schiff, K. Jerger, D. H. Duong, T. Chang, M. L. Spano, and W. L. Ditto, Nature (London) **370**, 615 (1994).

[8] D. Auerbach, C. Grebogi, E. Ott, and J. A. Yorke, Phys. Rev. Lett. **69**, 3479 (1992).

[9] F. J. Romerias, C. Grebogi, E. Ott, and W. P. Dayawansa, Physica (Amsterdam) **58D**, 165 (1992).

[10] V. Petrov, E. Mihaliuk, S. K. Scott, and K. Showalter, Phys. Rev. E **51**, 3988 (1995).

[11] A. De Wit, G. Dewel, and P. Borckmans, Phys. Rev. E **48**, R4191 (1993).

[12] P. Gray and S. K. Scott, Chem. Eng. Sci. **39**, 1087 (1984).

[13] W. N. Reynolds, J. E. Pearson, and S. Ponce-Dawson, Phys. Rev. Lett. **72**, 2797 (1994); V. Petrov, S. K. Scott, and K. Showalter, Philos. Trans. R. Soc. London A **443**, 631 (1994).

[14] L. Ljung, *System Identification—Theory for the User* (Prentice-Hall, Englewood Cliffs, NJ, 1984).

[15] G. C. Goodwin and K. S. Sin, *Adaptive Filtering, Prediction, and Control* (Prentice-Hall, Englewood Cliffs, NJ, 1984).

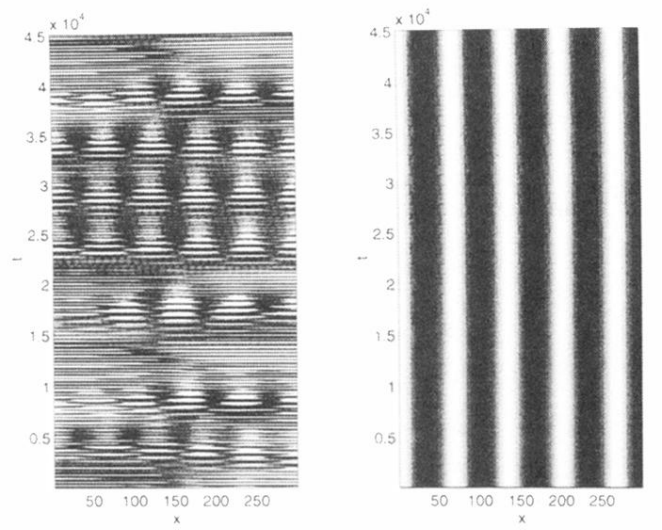

FIG. 4. Space-time plot of autonomous (left) and controlled (right) Gray-Scott system at $T_{\text{res}} = 214.5$.